

# CLEAR: Robust Context-Guided Generative Lighting Estimation for Mobile Augmented Reality

YIQIN ZHAO, Worcester Polytechnic Institute, USA

MALLESHAM DASARI, Northeastern University, USA

TIAN GUO, Worcester Polytechnic Institute, USA

High-quality environment lighting is the foundation of creating immersive user experiences in mobile augmented reality (AR) applications. However, achieving visually coherent environment lighting estimation for Mobile AR is challenging due to several key limitations associated with AR device sensing capabilities, including limitations in device camera FoV and pixel dynamic ranges. Recent advancements in generative AI, which can generate high-quality images from different types of prompts, including texts and images, present a potential solution for high-quality lighting estimation. Still, to effectively use generative image diffusion models, we must address their key limitations of generation hallucination and slow inference process. To do so, in this work, we design and implement a generative lighting estimation system called CLEAR that can produce high-quality and diverse environment maps in the format of 360° images. Specifically, we design a two-step generation pipeline guided by AR environment context data to ensure the results follow physical environment visual context and color appearances. To improve the estimation robustness under different lighting conditions, we design a real-time refinement component to adjust lighting estimation results on AR devices. To train and test our generative models, we curate a large-scale environment lighting estimation dataset with diverse lighting conditions. Through quantitative evaluation and user study, we show that CLEAR outperforms state-of-the-art lighting estimation methods on both estimation accuracy and robustness. In particular, CLEAR achieves 56% - 51% (an average of 53%) accuracy improvement on virtual object renderings across objects with three distinctive types of materials over different reflective properties. Moreover, CLEAR supports real-time refinement of lighting estimation results, ensuring robust and timely environment lighting updates for AR applications. Our end-to-end generative estimation takes as fast as 3.2 seconds, outperforming state-of-the-art methods by 110×.

CCS Concepts: • **Computing methodologies** → **Mixed / augmented reality**; • **Human-centered computing** → **Ubiquitous and mobile computing systems and tools**.

Additional Key Words and Phrases: mobile augmented reality; lighting estimation; generative model

## 1 INTRODUCTION

As new augmented reality (AR) hardware and software enter consumer markets, mobile AR technologies have positively impacted various industries, including e-commerce, education, and engineering [10, 32]. The growing public adoption of AR technologies demands new standards for content quality and application user experiences, particularly emphasizing the need for *visual coherency* between virtual and physical content to ensure high-quality user experiences. To create visual coherency, AR applications require an accurate and robust environment *lighting estimation*, which ensures that virtual objects blend naturally with the physical environment.

We define the lighting estimation task for AR systems as estimating a complete environment map (a 360° HDR image) from partial observation of the environment (an LDR image with limited FoV) in real-time. This task is critical for supporting three key aspects of photorealistic rendering in real-time AR systems. (i) Reflective object rendering, which requires a complete environment map with visually coherent details. (ii) Highlights and shadows rendering, which requires HDR pixel information in environment maps. (iii) Temporally consistent visual coherency, which requires the system to robustly adapt to changing environmental lighting in real-time.

To address this challenging task, traditional systems adopt autoregressive models [50]. These models extract low-frequency information based on camera input (shown in Fig. 1a). While these methods are able to capture

---

Authors' addresses: Yiqin Zhao, Worcester Polytechnic Institute, 100 Institute Road, Worcester, MA, USA, yzhao11@wpi.edu; Mallesham Dasari, Northeastern University, 360 Huntington Ave, Boston, MA, USA, m.dasari@northeastern.edu; Tian Guo, Worcester Polytechnic Institute, 100 Institute Road, Worcester, MA, USA, tian@wpi.edu.

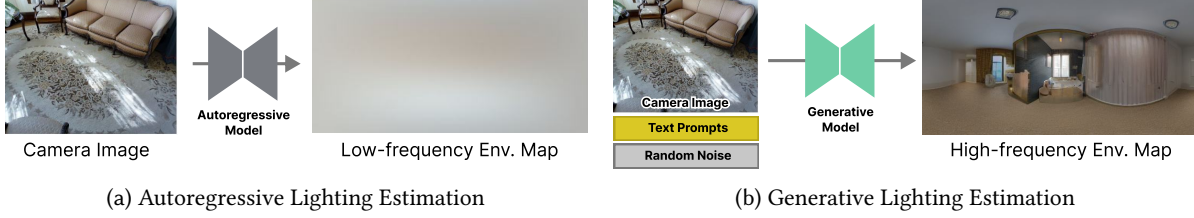


Fig. 1. Comparison between autoregressive and generative lighting estimation methods. (1a) An autoregressive lighting estimation system, Xihe [50], estimates omnidirectional low-frequency lighting information from camera images with autoregressive models. The low-frequency lighting information misses important visual details, as visualized in the example environment map. (1b) Generative lighting estimation models can create high-frequency environment lighting estimation results from limited environment observations. The estimation process can be conditioned in several ways, such as partial environment observations and text prompts.

coarse information about environmental lighting conditions, high-frequency details are missing. These details are important for creating a visually coherent AR system. To obtain the details, recent works [37, 41, 44] leverage the advancement of controllable generative models. These models have the potential to extract fine-grained environment details (shown in Fig. 1a), empowering AR systems with a better rendering effect. While generative-model-based methods seem promising, we identify two key challenges in using them on mobile AR systems.

First, robust lighting estimation demands accurate estimation under challenging lighting conditions. However, through a measurement study on existing datasets, we found that existing lighting estimation datasets have several distribution biases in key lighting properties, including light intensity and color temperatures. In further tests, we found that these data biases will affect the generalization and robustness of multiple recent lighting estimation models [3, 41]. Therefore, data diversity and fairness must be ensured when training and testing generative lighting estimation systems. Second, interactive mobile AR applications demand timely updates of lighting estimation results. However, generative models usually experience long inference latency. Without system latency optimization, naively integrating generative lighting estimation models into AR applications can easily violate the temporal constituency of immersive user experiences.

In this paper, we address the above issues with CLEAR, an edge-assisted novel generative lighting estimation system for mobile AR. To tackle AR device limitations in observation capability, we first design a *two-step generative pipeline* that estimates 360° HDR environment maps from partial LDR environment observations. Our key design insight is to separate the generative model training objective into two domains: *LDR environment map completion* and *high-intensity pixel value estimation*. This novel learning objective design addresses the practical challenges of the scarcity of high-quality lighting estimation training data, and allows us to leverage pre-trained large model to tackle each generation step effectively.

On top of the two-stepped generative pipeline, CLEAR uses controlling signals extracted from *AR context data* to ensure the estimated environment map aligns with the environment of physical AR devices. Specifically, CLEAR uses environment semantic maps, which control the environment map visual details, and device ambient light sensor data, which informs the lighting intensity and color temperatures during generation. Specifically, this information is used as image and text inputs for ControlNet models. This design helps the generative pipeline to handle the significant information increases during environment map generation.

Generative model inference latency is high, even on the edge servers. Therefore, we design an edge-device collaborative estimation system architecture with on-device refinement components to adjust edge estimation results to real-time lighting conditions. Specifically, we design a multi-output estimation strategy with an on-device adaptive output selection component. The estimation strategy is configured with the optimal number of generation outputs based on our performance measurement results. Additionally, CLEAR uses a color appearance

matching technique to efficiently and effectively adjust edge estimation results, even for challenging environment lighting conditions.

To evaluate the lighting estimation quality of CLEAR, we integrate CLEAR into a mobile AR application using Unity, Python, and a recent AR data streaming framework ARFlow [51]. We compare CLEAR’s virtual object rendering quality to ones using environment lighting acquired from three representative baselines: unwrapping a mirror ball (physical reference) [12], ARKit [4] (commercial), and LitAR [52] (academic). Our evaluation shows that CLEAR can generate environment maps with better image details to support more visually coherent virtual object rendering. To quantitatively understand CLEAR’s performance, we evaluate CLEAR with standard testing dataset [30] and compare with state-of-the-art lighting estimation models [3, 16, 30, 41]. Our evaluation shows that CLEAR outperforms DiffusionLight [30] by up to 56% using the three-sphere evaluation protocol [41]. Also, notably, CLEAR achieves 110X estimation latency reduction compared to DiffusionLight due to our efficient generative pipeline and generation control design. Furthermore, we verify the robustness of CLEAR under different lighting conditions by testing CLEAR on an augmented Laval dataset with diverse lighting conditions of light intensity and color temperatures. Qualitatively, our user study also confirms the effectiveness and robustness of CLEAR, which shows at least 12% higher quality ratings.

Related works on mobile AR lighting estimation systems seek to extract environment information from physical light probes [31], user dynamics, and learning-based solutions [17, 41, 44, 50]. While physical light probes provide the most comprehensive environment observations, their use in practical applications is typically constrained due to the need for physical light probe presence. While environment lighting can also be extracted from dynamic environment observations, the estimation is usually incomplete as AR devices often do not have comprehensive environment observations. In contrast, leveraging learned models to estimate environment lighting from AR device camera images is a more feasible solution for AR applications. Over the past couple of decades, learning-based methods have evolved from discovering scene lighting cues from image details, such as highlights and shadows [45], to regress omnidirectional environment lighting representations [17, 49, 50]. However, autoregressive models cannot effectively tackle the environment information generation in lighting estimation. For example, Xihe [50] provides real-time low-frequency lighting estimation to AR applications but fails to support detailed environment reflections on object rendering. More recently, a new opportunity has arisen as generative models can support highly detailed image content for environment map estimation [41, 44]. In this work, we focus on novel AR system integrations with image-generative models to provide high-quality environment lighting estimation. We specifically focus on adapting generative lighting estimation models to achieve robust estimation under challenging environmental lighting conditions.

We summarize our main contribution as the following:

- We design and implement a novel AR context-guided generative lighting estimation system, CLEAR. Our design leverages generative models to tackle the environmental observation limitation of AR devices. Specifically, our system uses a novel two-step generative lighting estimation pipeline to estimate an accurate environment map with visual details that match the AR user’s physical environment. To train the generative models, we craft a large-scale lighting estimation dataset with approximately 30K data items.
- We present a measurement study on recent lighting estimation datasets to understand the complexity of environmental lighting conditions and explore the challenges of achieving robust lighting estimation. With the insights from this study, we design and conduct lighting estimation robustness testing experiments to evaluate several lighting estimation systems, including ours.
- We develop two real-time estimation refinement techniques to improve the estimation quality of our system. Our first refinement component can automatically select the best environment map from generated results to match the current lighting conditions. Our second refinement component can match the color appearances between generated environment maps with real-time camera view to improve estimation robustness.

- We implement CLEAR as an end-to-end edge-assisted framework that can be integrated into third-party AR applications. We demonstrate the integration with an example object placement-based AR application. We will provide the dataset, system source code, and demo application links once the paper is accepted for publication to encourage follow-up research.
- We conduct comprehensive experiments to evaluate the effectiveness of CLEAR. Specifically, we tested CLEAR with SoTA lighting estimation systems on standard testing datasets and our robustness testing dataset. We also conduct a quality assessment study with human perception feedback on the lighting estimation results. Overall, the CLEAR rating score ranked the top with 12% higher than the second best method. Additionally, the overall standard deviation of the rating values for CLEAR is also lower than the second best method (1.67) by 7%.

## 2 BACKGROUND

**Lighting Estimation in Mobile AR.** Environmental lighting provides important environmental information and plays a crucial role in creating photorealistic visual effects when compositing virtual objects into real-world backgrounds [3]. Lighting estimation has been a long-standing research question in the vision and graphics community [26]. On mobile AR, estimating accurate environment lighting is important for creating immersive visual experiences when overlaying virtual content on physical environments. Such application includes virtual try-ons [48] and interactive games [35]. Obtaining accurate environment lighting on mobile AR faces several additional challenges compared to traditional image—or video-based lighting estimation tasks. For example, mobile AR devices usually have limited camera observation ranges, i.e., FoV. Because visually coherent AR experiences demand omnidirectional environment lighting, such camera observation capability limitation makes lighting estimation on mobile AR a highly ambiguous process and, thus, an ill-posed problem. Solving such problems typically requires a long computation time, while mobile AR applications demand timely environment lighting updates to maintain visual coherency in temporally changing lighting. To tackle these challenges, mobile system researchers typically aim to acquire environment information by leveraging spatial-temporal 3D environment observations [50] or guided user movements [52]. While increased environmental observation positively impacts the accuracy of lighting estimation, it does not sufficiently ensure the robustness of the results.

**Conditional Generative Models.** Recently, generative models have demonstrated impressive capabilities in high-quality data synthesis [11, 44]. Generative models have demonstrated impressive capabilities in high-quality data synthesis. Traditional generative models, such as Generative Adversarial Networks (GANs) [18], Variational Autoencoders (VAEs) [23], and autoregressive models [40], have demonstrated success in generating realistic images, text, and other types of data. However, these models are typically unconditional, meaning that they generate data without external guidance or specific control over certain attributes of the output. Conditional generative models extend generative models by incorporating additional information, referred to as conditions, to guide the generation process. These conditions can range from class labels in image generation [27] to textual descriptions in text-to-image models [33] or even semantic features for structured data generation [20]. In this work, we leverage ControlNet [46], a state-of-the-art conditional diffusion model, to implement context-guided generative lighting estimation. ControlNet allows conditional image generation from several conditioning sources, such as text, incomplete images, semantic maps, depth maps, key points, and edge maps. Our research leverages ControlNet’s conditional capabilities to incorporate rich and diverse information embedded in the AR context. Specifically, we explore how partial environment RGB observation, environment semantic map, and ambient lighting conditions can be effectively integrated into ControlNet to enhance immersive AR experiences.



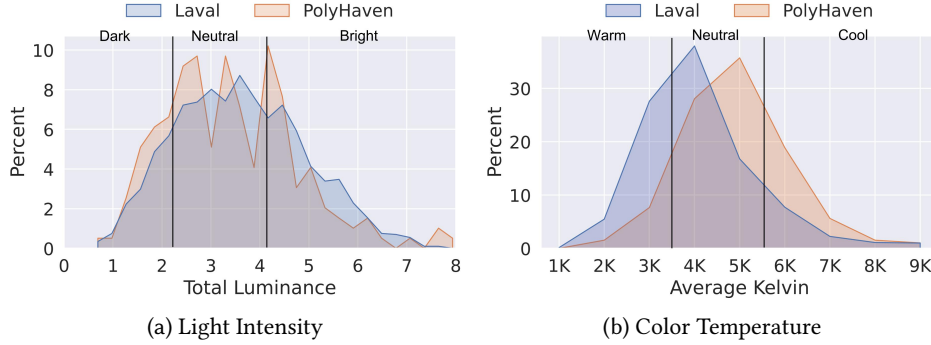


Fig. 2. Lighting condition measurement. We measure the distributions of light intensity (2a) and color temperature (2b) on environment maps collected from the Laval indoor dataset and PolyHaven. While both datasets include diverse lighting conditions, we observe several distribution biases in the datasets. For example, a significant part of the PolyHaven data items lies in the cool color range. Also, both datasets have an imbalanced distribution between neutral and other lighting conditions.

### 3 MOTIVATION AND CHALLENGES

We study the challenges of robust mobile AR lighting estimation through a measurement study. In §3.1, we explore the complexity of environment lighting conditions and the pre-existing biases in existing lighting estimation datasets. Then, in §3.2, we formally summarize the challenges.

#### 3.1 Lighting Condition Measurement

To understand the challenges in robust lighting estimation, we first conduct a measurement study of environmental lighting conditions on standard lighting estimation datasets. Our measurement focuses on two properties of environmental lighting conditions: *light intensity* and *color temperature*, representing an environment’s overall brightness and color appearances. We choose these two lighting condition properties because of their significant impact on virtual object rendering of all materials kinds [52]. We select two standard lighting estimation data sources: the *Laval dataset* [16], an academic open research dataset, and the *PolyHaven* website [1], a royalty-free HDR environment map data website. In total, we collected 2235 and 196 data items from the Laval dataset and PolyHaven, respectively. Following [30, 41], we perform a standard data preprocessing procedure of a color correction process with gamma correction with  $\gamma = 2.4$  and setting the 99th percentile of pixel intensity to 0.9.

Next, we calculate the properties of the lighting condition. We calculate the *light intensity* as the total luminance of a given HDR environment map image. To do so, we first calculate the individual pixel luminance  $l$ , which converts the original environment map image from RGB color space to the CIE XYZ color space [21] and then derives the pixel luminance component. We derive the total image luminance by summing the pixel luminance  $l$  weighted by their differential solid angles  $d\omega_i$  throughout the HDR environment map image:

$$L = \sum_{i=1}^N (0.212671R_i + 0.71516G_i + 0.072169B_i) d\omega_i \quad (1)$$

where  $i$  represents the  $i$ -th pixel in the environment map with  $N$  pixels. For color temperature value extraction, we first calculate the average pixel RGB value from each environment map and then calculate its correlated color temperature using a recent method [29]. The calculated environment map image color temperature values are given in the Kelvin unit. In Figure 2, we visualize the measured lighting condition distributions and annotate the human-perceivable categories of the light intensity and color temperature conditions. While both datasets contain a wide selection of lighting conditions, the data distribution shows several biases. Predominantly, neutral

lighting conditions of light intensity and color temperatures are seen in two datasets. For light intensity, more low-light environments than bright-lighting conditions data items are seen in the Laval dataset. As for the color temperature distribution, a significant part of the PolyHaven data items lies in the cool color range. These data distribution biases have also led to biased training and evaluation of lighting estimation systems. In particular, we will show robustness testing results of several recent lighting estimation models in §6.

### 3.2 Robust Lighting Estimation Challenges

Here, we summarize two key challenges in designing a robust mobile AR lighting estimation system.

**3.2.1 Diverse Lighting Conditions.** As our measurement study suggests, real-world environment lighting has complex physical properties, such as light intensity and color temperatures. Achieving accurate results in diverse lighting conditions requires estimation systems to match the estimated environment map color profiles to the lighting conditions while maintaining the estimated environment image visual details. This requirement demands lighting estimation systems to have rich built-in knowledge of diverse environmental lighting conditions. Additionally, as mobile AR devices only have limited environment observation, estimating high-quality environment maps requires lighting estimation systems to complete an omnidirectional environment view based on existing observations. This inherently ambiguous process demands the system to create visual contexts that closely match the physical surroundings of the AR user, while accurately estimating high-intensity light sources to ensure realistic rendering of highlights and shadows on virtual objects. Moreover, real-world environmental lighting conditions often vary from scene to scene and from time to time. For example, indoor rooms with daytime sunlight usually appear in neutral color temperatures, while rooms lit with LED light sources can appear in either warm or cold colors. To ensure the consistency of mobile AR visual experiences, lighting estimation systems must also adapt their estimation results to changing environment lighting conditions in real-time.

**3.2.2 Data Availability and Biases.** Our measurement study also shows that existing standard lighting estimation datasets do not have a balanced light intensity distribution or color temperatures. When used to train lighting estimation models, these data biases can lead to model generalization issues in underrepresented lighting conditions. Furthermore, the availability of high-quality HDR lighting estimation datasets is extremely limited. To capture a high-quality HDR environment map, researchers usually need to use a professional DSLR camera to take multiple images of the environment at different angles and under different camera exposures [12]. This process can be costly and time-consuming. Even in cases where professional setups can be created for lighting ground truth capturing, it is still impractical to capture a dataset that contains comprehensive lighting conditions and environmental details. Additionally, these data biases can also make it difficult to conduct fair evaluations to test the robustness of existing lighting estimation systems. As a result, current lighting estimations often overlook the importance of robustness under different lighting conditions and fail to adapt to the complex real-world environments of mobile AR users.

## 4 CLEAR DESIGN

### 4.1 Overview

We design CLEAR to tackle the abovementioned challenges and provide *robust and high-quality HDR environment maps* for mobile AR. The design of CLEAR leverages the recent advancement of generative models [46], which can better integrate with rich conditioning inputs to ensure appropriate image context on the generated environment maps. In contrast to prior works that focus on generative model architectures [3, 16, 30, 41], the core of CLEAR lies in the novel integration between image generative models and AR systems to ensure high-quality and robust generative lighting estimation. Specifically, CLEAR uses a context-guided generative lighting estimation pipeline (§4.2) that incorporates mobile AR context information to estimate visually coherent environment

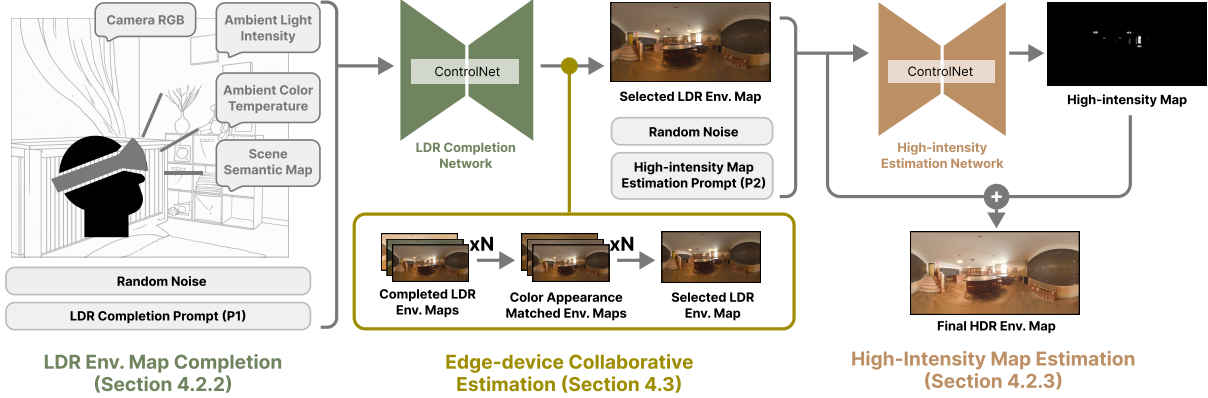


Fig. 3. Overview of CLEAR. CLEAR uses several types of AR context data to guide a two-step high-quality lighting estimation pipeline. The first step (§4.2.1) completes partial environment observations in the LDR pixel range domain. The completed environment maps will be post-processed and selected with our adaptive estimation control and refinement components (§4.3) and given to the following high-intensity map estimation step (§4.2.2). Finally, CLEAR outputs an HDR environment map by combining the completed LDR environment map and the high-intensity map.

maps. Additionally, CLEAR uses an edge-device collaborative estimation architecture (§4.3) to allow robust and temporally consistent lighting estimation. On the edge, we leverage a multi-output estimation strategy (§4.3.1) to tackle the inherent ambiguity of generative models in environment lighting estimation. On the client, we design several techniques to effectively select and refine (§4.3.2) edge-estimated environment maps to match real-time environment lighting conditions observed on the AR device.

## 4.2 Context-Guided Generative Lighting Estimation

Estimating HDR omnidirectional lighting from limited LDR environment observations is a process that requires significantly increased information. While generative models are good at such tasks, properly controlling the generation process is critical to ensure accurate results when generating environmental lighting. Our key insight to address this issue is *leveraging AR context data to control the generation*. Figure 3 shows an overview of our context-guided generative lighting estimation pipeline.

**4.2.1 LDR Environment Map Completion.** CLEAR completes the environment map from limited camera observations in the LDR image pixel ranges at the first step. Here, we follow the standard image format convention and consider the pixel range between  $[0, 255]$  as the LDR pixel range. To achieve the LDR completion, we leverage ControlNet [46] and pre-trained StableDiffusion [34] models to train controllable image generative models. We chose ControlNet because it provides flexible controllability in image generation with text and image conditioning data that can be naturally integrated with the AR context. The pre-trained StableDiffusion model provides embedded image generation knowledge learned from large-scale image generation datasets<sup>1</sup>. While the pre-trained large models can natively generate diverse images, they must be fine-tuned to output the correct environment map content and styles. To fine-tune the completion model, we generated approximately 30K data items from online sources. The data collection and generation processes will be described in §5.

<sup>1</sup>Note that CLEAR’s design is not tied to ControlNet nor StableDiffusion, and that means other conditional image generative models can serve as drop-in replacements to improve the performance of CLEAR in the future.

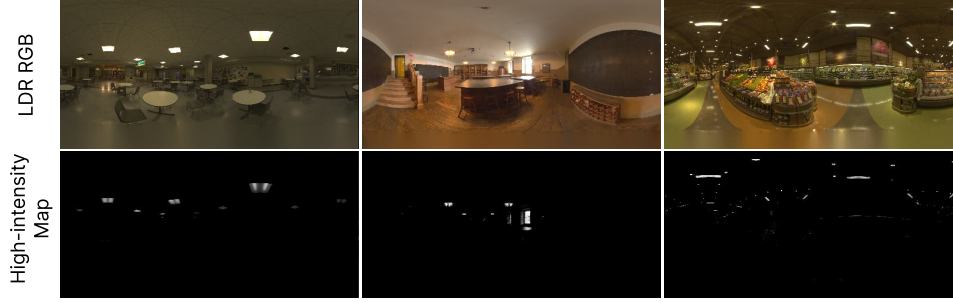


Fig. 4. Visualization of high-intensity pixels. We decompose three examples of HDR environment maps into an LDR RGB component (row 1) and a high-intensity component (row 2). The high-intensity pixels, i.e., bright light spots on the environment map, are extracted using Equation (2).

In the completion process, we provide the ControlNet with camera RGB observations and scene semantics as image conditioning inputs and encode ambient light intensity and color temperatures in the text conditioning input. For camera RGB observations, we stitch multi-view camera RGBs into 360 ° panoramic environment map images in advance. Note that this design can be extended with more sophisticated environment reconstruction methods like [52] or combined with multi-user environment observation sharing to increase the observed environments. The environment semantic map is also processed into 360 ° panoramic images as a ControlNet input. We follow the ADE20K [54] definition and use 150 instance labels in the semantic map data.

For encoding ambient lighting condition data, we convert numerical lighting condition data into words describing the lighting condition’s characteristics. We use the following text prompt template to describe ambient lighting conditions. We create the ambient light property labels based on partial environment map image pixels with empirically derived threshold values. The light intensity label is defined by the mean pixel intensity calculated from Equation (1) with values between 0.25 and 0.40 as *neutral*, and the rest values as *dark* and *bright*. The color temperature label is defined by the mean pixel color temperature with values between 3500K and 5500K as *neutral*, and the rest values as *warm* and *cool* [28]. The lighting condition words are marked in bold font.

**P1:** A panoramic photo of an indoor room. The room is in a [**dark/neutral/bright**] lighting condition. The room has a [**warm/neutral/cool**] ambient color.

**4.2.2 High-intensity Map Estimation.** In Figure 4, we show examples of environment map high-intensity components (high-intensity map). The high-intensity components describe environment light intensities and directionalities, which are critical for rendering photorealistic highlight and shadow effects on AR objects. However, due to the device’s camera imaging capability, this information often cannot be directly captured by mobile AR devices. Thus, it is important to estimate high-intensity environment components from LDR environment observations.

Similar to the completion of the LDR environment map, we utilize an image generation model to generate high-intensity maps based on the LDR completion results. The key challenge to building a high-intensity map estimation model is data scarcity. Specifically, existing high-quality HDR environment map data are very limited. For example, the Laval dataset only includes approximately 2K data items. Training generative models on small datasets can be highly unreliable. Additionally, pre-trained backbone models, like StableDiffusion [34], cannot be directly leveraged because they are trained on LDR images.

To address these challenges, we propose a novel learning formulation to allow high-intensity estimation in the LDR pixel range domain. Specifically, our design includes two key steps. First, we use a scaling transformation to convert HDR environment maps into LDR and high-intensity maps, like the examples in Figure 4. We define the

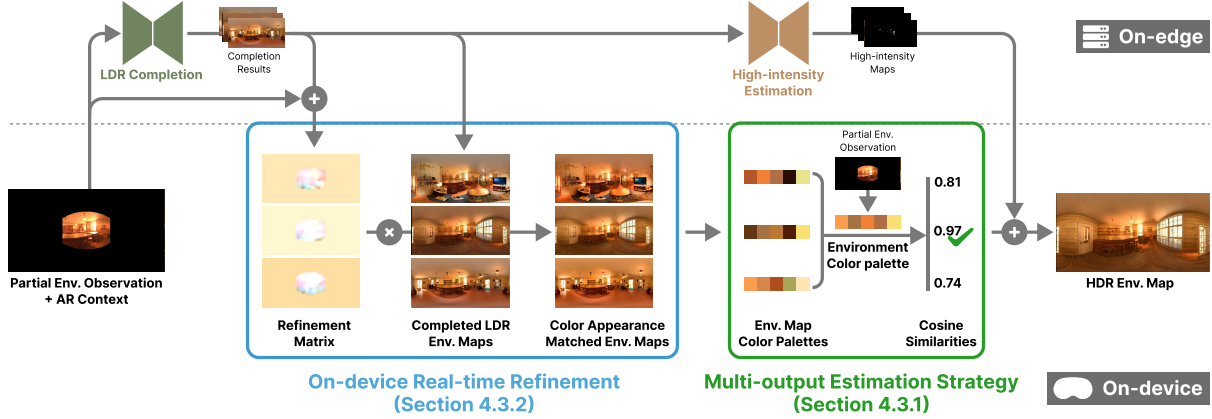


Fig. 5. Estimation refinement workflow. CLEAR uses a hybrid architecture to offload heavy generative model inference to the edge server while adaptively refining estimation results on AR devices in real time. We adopt a multi-output estimation strategy to tackle the estimation ambiguity (§4.3.1). On the client, our system first matches the color appearances between the completed environment maps to the real-time camera observations (§4.3.2). This operation helps improve estimation accuracy in challenging lighting conditions and enables real-time adaption of the generative estimation result. Here, we show the refinement process for an extremely cool environment lighting temperature condition to highlight the importance of color appearance matching. Then, our system client chooses the best estimation result based on real-time environment observation. The chosen environment map is combined with its corresponding high-intensity map estimation to create the final HDR environment map for AR virtual object rendering.

high-intensity map as a 360° image that describes the high-intensity light positions, directions, and high-intensity pixel values. In particular, the high-intensity map is also an LDR image where the pixels describe the intensity exponent of the original HDR image pixels. we use Equation (2) to implement the conversion.

$$I_m = 2.0 / (1 + e^{-I_i}) - 1.0 \quad (2)$$

Then, we fine-tune a pre-trained generative model to learn the generative process of generating high-intensity maps from LDR environment maps. We can use pre-trained generative models for this task because the input and output image pixels are in the LDR range. More importantly, the high-intensity values are strongly associated with simple LDR image features, such as bright spots and light strips, making the high-intensity map estimation task relatively simple compared to the LDR completion task. This novel design allows us to overcome the HDR data availability challenge and use the small amount of ground-truth HDR data from the Laval dataset to train the high-intensity estimation model. During training and inference, we also supply the following text prompt to provide quality conditions to the high-intensity estimation process:

**P2:** *A grayscale panoramic image describing the bright spots of an indoor room. Brighter spots get more bright color. Regions without light sources should stay pure black.*

The prompt guides the high-intensity map estimation model in generating the correct image style, outputting consistency in high-intensity estimation, and helping to reduce visual artifacts in the estimated results. Combined with the completed LDR environment map from the first step (§4.2.1), our generative lighting estimation pipeline outputs a 360° HDR environment map.





Fig. 6. Examples of color appearance refinement. We use examples of extreme lighting conditions, extremely cool temperature (row 1) and extremely warm temperature (row 2), to show how our color refinement algorithm can improve the estimation result color accuracy. Compared to the original LDR completion result, our refined environment map color is closer to the original full environment map (marked as Reference). Columns 5 and 6 show additional results to visualize the effects of median blur filtering and patch splitting on the refinement results. Particularly, visual artifacts can be observed on the image regions between the transitioning edges of the observed and unobserved environments.

### 4.3 Edge-device Collaborative Estimation

Robust mobile AR lighting estimation requires accurate and timely estimation result updates to address the changing environmental lighting. However, providing real-time generative estimation on AR devices is impractical due to the high inference latency of generative models. Therefore, we adopt an edge-device collaborative estimation architecture design similar to recent works [5, 50]. Figure 5 illustrates the collaborative estimation process. Specifically, we utilize a multi-output estimation strategy (§4.3.1) to tackle the estimation ambiguity problem. And, on the client, CLEAR selects and refines the best environment map on the AR device based on real-time environment observations (§4.3.2).

**4.3.1 Multi-output Estimation Strategy.** Completing 360° environment maps from low-FoV environment observations is inherently ambiguous. To tackle this problem, we utilize a multi-output estimation strategy. The key insight of this strategy is to generate multiple completion variants and match the best one to real-time environment observations. The process can be described in three steps. First, CLEAR uses different random seeds on the edge to adjust LDR completion ControlNet to output different completion results. After the CLEAR client receives the completion results, the client first refines the completed environment map colors (§4.3.2). Finally, it utilizes another step on the client to match the best completion result to real-time environment observations. Specifically, our matching technique first creates color palettes from the observation and estimation environment map images. The color palettes are selected via the K-means algorithm by finding the five most common colors for each environment map image. The selected colors are profiles of each environment map. Then, our method calculates a cosine similarity between the observed and estimated environment map palettes and finds the best environment map for the current environment lighting. The total cosine similarity is calculated as the sum of per-color cosine similarity between color palettes.

**4.3.2 On-device Real-time Refinement.** Addressing unpredictable changing environment lighting is crucial for supporting temporally consistent AR object rendering. To address this challenge, CLEAR uses a lightweight on-device refinement technique to refine the multi-output LDR completion results to align with the real-time environment observations. Specifically, our technique seeks to create a color refinement matrix of pixel color multipliers for the completed LDR environment maps. The color refinement matrix consists of two types of multiplier values: (i) the global color multiplier and (ii) the local color multiplier. The global color multiplier adjusts the overall image colors of completed environment map images, while the local color multiplier adjusts fine-grained colors on the observed environment map regions.

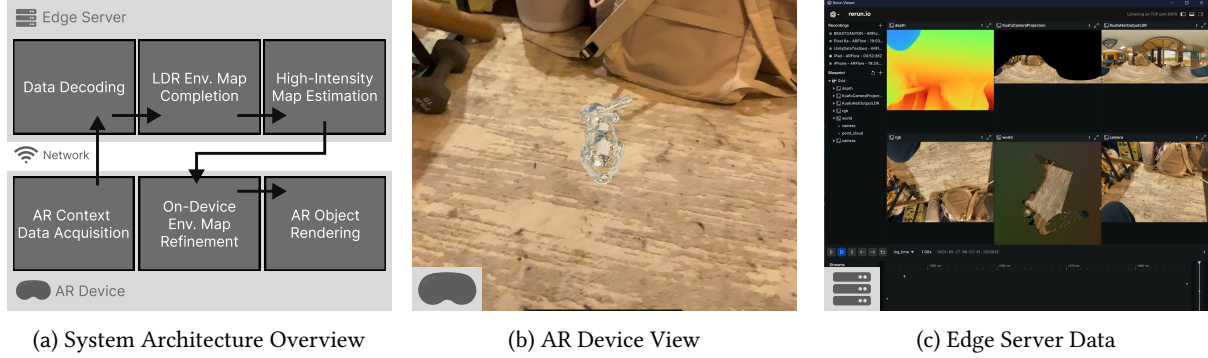


Fig. 7. System implementation and AR application integration. **7a** An overview of the software components of CLEAR. **7b** An AR application screenshot of a rendered virtual bunny with CLEAR estimated environment lighting. **7c** The device uploaded AR data to the edge server.

Our technique calculates the global color multiplier by deriving per-channel multipliers as the ratio between average colors in the estimated and observed environment map images. The local multipliers are calculated by first splitting the estimated environment map images and the partial environment observation image into  $N \times M$  patches. Then, our technique calculates local multipliers as the average color ratios for each patch. Finally, the two color refinement terms are combined into a color refinement matrix. The calculated local multipliers for environment map regions with observed environment pixels and the global multiplier for others. A  $3 \times 3$  median blur filter is used to address color smoothness between the observation edges. Empirically, we found  $8 \times 8$  is the best image patch size. As shown in Figure 6, our refinement technique can adjust environment map colors even in very challenging lighting conditions.

## 5 IMPLEMENTATIONS

### 5.1 System Implementation

We implement CLEAR based on a recent AR data streaming framework, ARFlow [51], which enables low-latency bidirectional data streaming between our edge service and AR application client. CLEAR consists of a client-side and a server-side component. Figure 7 shows an overview of the CLEAR architecture. We implement the client as a Unity3D<sup>2</sup> package. The client is responsible for streaming and receiving mobile AR device data and providing AR applications with estimated environment maps. We use ARFlow’s built-in data collection feature to capture camera RGB, depth, and device tracking data provided by ARFoundation<sup>3</sup>, Unity’s low-level AR framework. The captured data is then streamed to our server via the ARFlow gRPC service. The server component is a Python-based service for the generative lighting estimation pipeline host and inference. On the server, we first decode and prepare the AR data into NumPy arrays. During generative model inference, we combine the RGB and semantics-guided ControlNet models using the MultiControlNet pipeline from the HuggingFace Diffusers<sup>4</sup> library. We configure the ControlNet model inference to use the UniPC [47] sampler with 20 steps. To accelerate inference speed, We include a specialized diffusion model optimization library xformers<sup>5</sup> to reduce the estimation latency. Our generative estimation pipeline outputs environment maps at  $512 \times 256$  resolution.

<sup>2</sup>Unity3D: <https://unity.com>

<sup>3</sup>ARFoundation: <https://docs.unity3d.com/Packages/com.unity.xr.arfoundation@6.0/>

<sup>4</sup>Diffusers: <https://huggingface.co/docs/diffusers>

<sup>5</sup>xFormers: <https://facebookresearch.github.io/xformers/>

## 5.2 Dataset Generation

**5.2.1 LDR Environment Map Completion Data.** We first collect a large set of LDR environment map images from two large LDR indoor environment map sources: the Matterport3D dataset [7] and Structured3D datasets [53]. The Matterport3D dataset provides a large set of real-world captured environment maps, and the Structured3D dataset provides a large set of synthetic environment map images with photorealistic visuals. The combined training dataset consists of 29461 data items, 10x larger than the Laval dataset [16].

Next, we mask the LDR environment map images at random angles to generate AR camera observation images. The masks are generated using the pin-hole camera model to simulate the real-world partial environment observations. We also combine multiple image masks to simulate multi-view environment observations. Specifically, the number of views is randomly chosen from 1 to 5, and the camera horizontal FoV is randomly chosen between 60 and 120 degrees. For environment semantics, we use a pre-trained semantic map estimation model [43] to estimate semantic maps directly from the collected LDR environment maps. We also use the LDR image mask to generate masked semantic maps representing environment semantic information received by AR devices. For the ambient lighting condition prompt generation, we create the ambient light property labels using the masked partial environment map image pixel values and our defined system threshold values in §4.2.1.

**5.2.2 High-intensity Map Estimation Data.** With our novel high-intensity map learning objective design, the high-intensity map estimation model can be fine-tuned with a small training data set. Therefore, we only use the Laval dataset’s training split to generate the high-intensity map estimation training data. In total, we created 1489 data pairs of LDR environment map images and high-intensity map images. To generate each data item, use Equation 2 to generate the data items. Specifically, we first clamp the raw HDR environment map into  $[1, +\infty]$  and then scale the results to  $[0, +\infty]$  to get a raw high-intensity map  $I_i$ . Next, we convert the range of the raw high-intensity  $[0, +\infty]$  to the standard LDR pixel range in  $[0, 1]$ . Note that although this transformation is not lossless, our evaluation suggests minimal impact on the overall lighting estimation. In addition to the generated image pair data, we add the text prompt **P2** during training.

## 5.3 Model Training

Our generative lighting estimation pipeline consists of three ControlNet [46] models, two for LDR environment map completion with RGB and semantics context, and one for high-intensity map estimation. We train all the models by fine-tuning the pre-trained StableDiffusion 1.5 inpaint [34] checkpoint. We apply several data augmentation techniques to the previously generated datasets to train the models and improve generalization in different lighting conditions and environmental contexts. We augment the lighting condition by applying a random scaling  $s$  similar to the scaling term used in the robustness test data generation. This augmentation is only applied to LDR environment map completion training. For environment context augmentation, we apply horizontal rotations to environment map images. This augmentation is used for both LDR completion and high-intensity map estimation training. Our generative lighting estimation models are trained on affordable commercial PC hardware, specifically, a high-end workstation PC with an I9-13900K CPU and an RTX4090 GPU. The LDR completion model requires an average of 12 hours of training, while the high-intensity map estimation model, due to its smaller training dataset, only requires an average of 4 hours.

## 6 EVALUATION

We evaluate the performance CLEAR using an AR application testbed, a set of data-driven benchmarks, and a user study. The testbed-based evaluation shows the real-world lighting estimation quality of CLEAR. It also allows us to profile and break down the system latency. The data-driven benchmarks evaluate the lighting estimation quality of CLEAR on several test datasets. To evaluate the robustness of CLEAR’s lighting estimation, we introduce

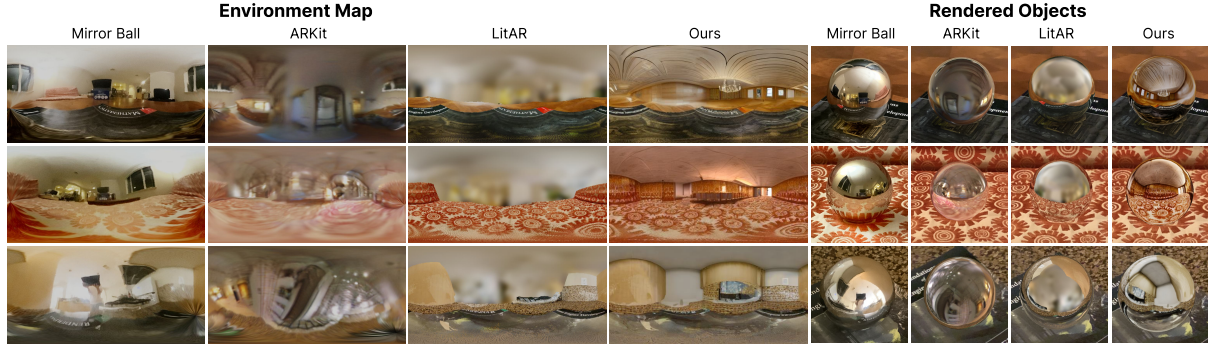


Fig. 8. AR object rendering results. We show AR virtual object rendering qualitative comparison to other environment lighting acquired by unwrapping a physical mirror ball [12] (reference), ARKit [4] (commercial), and LitAR [52] (academic). Compared to ARKit, CLEAR estimates the environment map with significantly more realistic visual details. Compared to LitAR, CLEAR can generate more visually coherent far-field environment map details, while LitAR can only generate blurry ones.

a new robustness testing protocol and a robustness testing dataset generated from the Laval dataset. The user study explores CLEAR lighting estimation quality from the perspective of human perception.

## 6.1 Testbed-Based Evaluation

**6.1.1 Testbed setup.** We implement a Unity-based cross-platform AR application to demonstrate the lighting estimation capability of CLEAR. Our application implements an object placement action that allows AR users to visualize 3D objects in their physical environment at selected locations. This demonstration application mimics the behaviors of virtual object staging applications and shows potential improvements in application visual quality. When using the application, users are requested to select an environment location to place objects based on on-screen visual instructions. After the object placement action, we request lighting estimation from CLEAR and apply the result environment map for object rendering.

**6.1.2 Qualitative Visual Comparison.** We implement a Unity-based cross-platform AR application to demonstrate the lighting estimation capability of CLEAR. Our application implements an object placement action that allows AR users to visualize 3D objects in their physical environment at selected locations. This demonstration application shows the potential impact of photorealistic rendering on immersive AR applications, such as AR shopping [22]. After the object placement action, we request lighting estimation from the testing lighting estimation system and apply the result environment map for object rendering in Unity. We followed the LitAR [52] experiment setup to compare lighting estimation system performance under three different scenes. In Figure 8, we compare between environment lighting acquired by unwrapping a physical mirror ball [12], LitAR [52], and ARKit [4]. The mirror ball captured environment map represents a reference physical environment lighting at the estimation position. To compare fairly to LitAR, we used the same near-field dense environment reconstruction data as our lighting estimation input. Overall, we observe that CLEAR outputs the best environment map image quality among estimated environment maps (ARKit and LitAR). CLEAR generates environment maps with more visual details than LitAR and fewer artifacts than ARKit. Particularly, CLEAR can generate detailed far-field environments while LitAR can only generate blurry ones. The improved environment map quality also helps more visually coherent virtual object rendering.

**6.1.3 System Performance Breakdown.** We conduct a comprehensive system profiling to quantify the system runtime latency. We measure the end-to-end system latency of CLEAR and other methods on a high-end



Table 1. System performance breakdown. We show the breakdown of system latency under different generative estimation settings for CLEAR. Our system can finish end-to-end environment map generation as fast as 2383ms. Under the default configuration, our system uses partial environment RGB in the inputs and generates five environment map completion results. The default estimation latency is 3269ms.

System Component	Avg. Time (ms)	End-to-end System	Avg. Time (ms)
Data preparation	12 ( $\pm 1.2$ )	LDR completion x1 (RGB)	2383 ( $\pm 11.4$ )
LDR completion x1 (RGB)	1130 ( $\pm 11.4$ )	LDR completion x1 (RGB + Semantics)	3021 ( $\pm 51.3$ )
LDR completion x3 (RGB)	1574 ( $\pm 17.6$ )	LDR completion x3 (RGB)	2825 ( $\pm 17.6$ )
LDR completion x5 (RGB)	2012 ( $\pm 19.5$ )	LDR completion x3 (RGB + Semantics)	4526 ( $\pm 31.5$ )
LDR completion x7 (RGB)	2492 ( $\pm 18.1$ )	LDR completion x5 (RGB)	3269 ( $\pm 19.5$ )
		LDR completion x5 (RGB + Semantics)	5855 ( $\pm 38.5$ )
Output processing	64 ( $\pm 9.2$ )	LDR completion x7 (RGB)	3741 ( $\pm 14.2$ )
HDR estimation x5	1166 ( $\pm 10.7$ )	LDR completion x7 (RGB + Semantics)	8082 ( $\pm 56.9$ )

workstation PC with an RTX 4090 GPU. In Table 1, we break down the end-to-end system latency measurement results. In the default configuration, CLEAR generates five LDR completion results. Overall, the end-to-end inference takes 3269ms, mostly consisting of the generative LDR completion time. When combined with semantics in LDR completion, our systems take 3269ms to generate five LDR environment map completion results. We observe that the main impact factor for the LDR completion process is the number of environment map outputs. We notice that increasing generation output introduces a near-linear yet slow increase in the estimation latency. Although our default system configuration uses five outputs, the estimation latency is only about double the time of using a single estimation output.

## 6.2 Data-Driven Evaluation

**6.2.1 Robustness Evaluation Data Generation.** Evaluating the robustness of lighting estimation systems is particularly challenging because it requires controlled lighting condition changes. To avoid costly real-time data capturing, we propose an image editing-based method that creates variants of standard lighting estimation testing datasets to represent diverse lighting conditions while maintaining the original environment map visual context. To do so, we use an informed augmentation selection-based method with the following three steps. First, we generate a set of edited variants of the Laval dataset by applying a uniform scaling term  $s$  to all environment map images. Then, we measure the total light intensity and average color temperatures using the measurement method introduced in §3. Finally, we sample a range of edited dataset variants by comparing the newly measured light intensity and color temperature values to the original values. The scaling term  $s$  are selected from  $[0.25, 4]$  using a step of 0.125. For the light-intensity editing, the scaling term is uniformly applied to all three color channels, while only red and blue channels are scaled with  $s$  and  $1/s$  for color temperature editing [2]. Figure 9 shows examples of the edited environment maps. We created a set of augmented Laval indoor datasets using this method with edited average light intensity and color temperatures in  $[-20\%, 20\%]$  and  $[-50\%, 50\%]$ .

**6.2.2 Experiment Setups.** To quantitatively evaluate the lighting estimation quality, we use several datasets and protocols to evaluate environment map estimation accuracy, diversity, and robustness. We use the original Laval dataset and our generated robustness testing datasets for the evaluation. We test our system against recent state-of-the-art lighting estimation models, including DiffusionLight [30], StyleLight [41], and OmniDreamer [3]. Among these baselines, DiffusionLight is the most similar to our method design because it uses a diffusion model-based pipeline for generating environment maps. Our experiment includes standard environment map evaluation on the Laval testing dataset. We also use two specialized experiment protocols to understand the





Fig. 9. Experiment protocol. Our experiment includes two protocols. For the three-sphere protocol (left), we use environment maps (middle) from the Laval dataset to render virtual spheres of different material properties. The rendered spheres provide us a proxy to understand the impact of lighting estimation results on virtual object rendering. We augment the Laval dataset to create diverse training and test data in different lighting conditions. We use the robustness testing protocol (right) to understand the robustness of lighting estimation results. We generate the robustness testing data by editing the Laval dataset environment maps’ ambient light intensity and color temperatures. In the example, we augment an environment map (middle) with four variants with different light intensities and color temperatures. The results (right) of light intensity augmentation are marked as *dark* and *bright*, and the results of color temperature augmentation are marked as *warm* and *cold*.

robustness of our lighting estimation results and the impact of lighting estimation on virtual object rendering. Specifically, we use the following two protocols to conduct our evaluation:

**The three-sphere protocol.** The three-sphere evaluation protocol [30, 41] is a proxy method to evaluate the HDR lighting estimation accuracy. The method evaluates the lighting estimation accuracy through pixel-wise error measurements on three rendered spheres with different material properties. Specifically, the used sphere materials are: *matte*, *silver matte*, and *silver*. Figure 9 shows a set of rendered virtual spheres used in this evaluation protocol. Each material represents a mixture of specific reflectance and roughness properties. Compared to direct environment map-wise comparison, this evaluation protocol helps us understand the *impact of lighting estimation results when applied to object rendering*.

**The robustness testing protocol.** We design an experiment protocol to test the *generalizability and robustness of lighting estimation systems* under different lighting conditions, specifically with different light intensity and color temperatures. In this protocol, we test lighting estimation systems on the previously generated robustness evaluation dataset. Then, we compare estimated environment maps with the ground truth and calculate pixel-wise errors. This protocol directly calculates pixel-wise errors on the LDR image domain because it focuses on the lighting condition-related color appearance differences between environment map images.

**Evaluation Metrics.** To quantify the quality of the generative lighting estimation pipeline, we evaluate the following aspects: (i) diversity of generated environment maps, and (ii) environment map estimation accuracy. Following previous research works [3, 17, 30, 41], we use the FID score [36] to measure the diversity of environment generation. For accuracy evaluation, we use three scale-invariant image-based metrics to evaluate lighting estimation accuracy on rendered virtual spheres: scale-invariant Root Mean Square Error (si-RMSE) [14], Angular Error [25], and normalized RMSE. For the last metric, we follow [30] to map the 0.1st and 99.9th value percentiles to 0 and 1. We apply these evaluation metrics to measure the lighting estimation quality on the LDR environment completion results and the final HDR environment map output.

**6.2.3 End-to-End Estimation.** In Figure 10, we show qualitative comparisons between CLEAR and competing methods in three scenes, representing the neutral, warm, and cool lighting conditions. For each set of comparisons

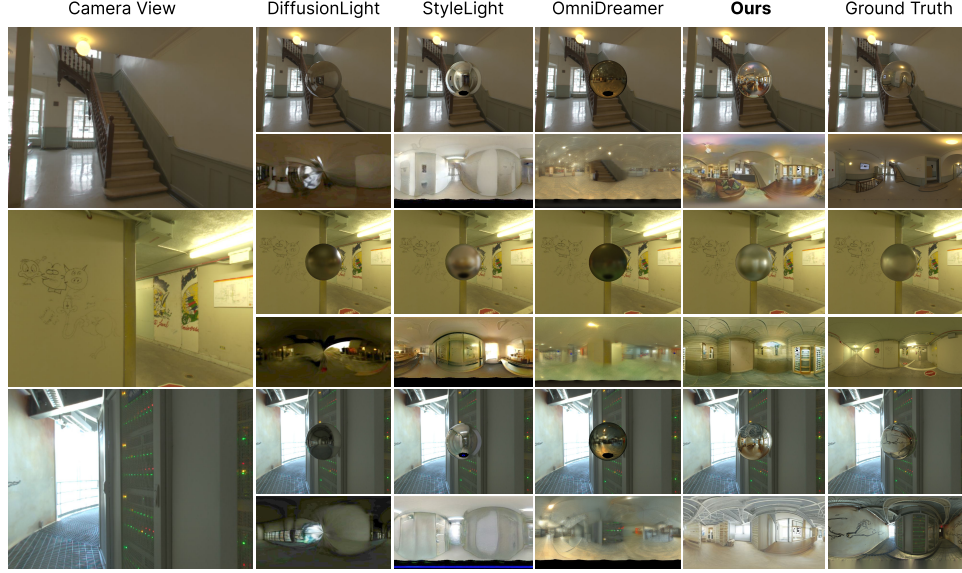


Fig. 10. Qualitative comparisons. We show examples of lighting estimation results on three scenes and the corresponding rendered virtual sphere images. On the left, we show the input camera view for lighting estimation systems. On the right, we show rendered virtual spheres (row top) and estimated environment maps (row bottom).

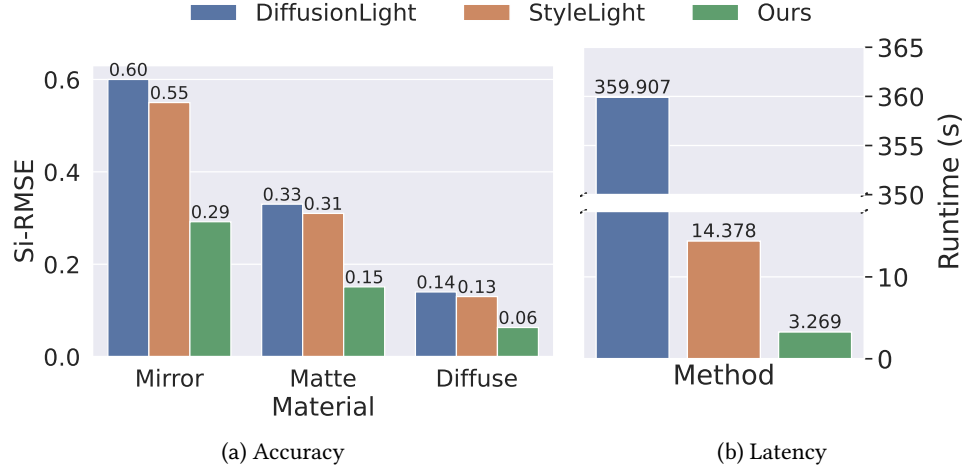


Fig. 11. End-to-end qualitative comparison. We compare the end-to-end estimation accuracy (11a) and estimation latency (11b) between CLEAR and two state-of-the-art works [30, 41]. Our method achieves the lowest estimation error on all three object material types in the three-sphere evaluation protocol. This indicates the lighting estimation results from our system can provide the best visual quality support for virtual object rendering. For estimation latency, our method significantly outperforms other generative model-based methods.

Table 2. Ablation evaluation on the three-sphere protocol. On the standard testing settings with single 75° camera view input (row 1 - 3), our system achieves leading accuracy when compared to StyleLight [41] and DiffusionLight [30] on the three-sphere evaluation protocol. More camera observations and environmental semantics will significantly reduce our system’s estimation error.

Method	Scale-invariant RMSE ↓			Angular Error ↓			Normalized RMSE ↓		
	Diffuse	Matte	Mirror	Diffuse	Matte	Mirror	Diffuse	Matte	Mirror
StyleLight [41]	0.13	0.31	0.55	4.24	4.74	6.78	0.23	0.40	0.51
DiffusionLight [30]	0.14	0.33	0.60	<b>2.14</b>	<b>3.42</b>	<b>5.94</b>	<u>0.20</u>	<u>0.36</u>	<u>0.43</u>
Ours w. RGB+semantics 75° FoV 1 view	<b>0.06</b>	<b>0.14</b>	<b>0.28</b>	4.41	5.91	8.89	<b>0.17</b>	<b>0.20</b>	<b>0.37</b>
Ours w. RGB+semantics 110° FoV 1 view	0.05	0.13	0.27	4.19	5.77	8.66	0.16	0.19	0.35
Ours w. RGB+semantics 110° FoV 3 views	0.03	0.10	0.24	3.89	5.21	8.23	0.13	0.17	0.31
Ours w. RGB+semantics 110° FoV 5 views	<u>0.02</u>	<u>0.09</u>	<u>0.22</u>	<u>3.71</u>	<u>5.13</u>	<u>8.17</u>	<u>0.11</u>	<u>0.16</u>	<u>0.29</u>
Ours w. RGB+full semantics 110° FoV 3 views	<b>0.02</b>	<b>0.07</b>	<b>0.20</b>	<b>3.59</b>	<b>4.96</b>	<b>8.09</b>	<b>0.10</b>	<b>0.15</b>	<b>0.27</b>

in the figure, we include the input camera view, estimated environment map, and rendered virtual spheres overlaid on the original camera view. The rendered virtual spheres are also examples of the three-sphere evaluation protocol. Compared to other methods, CLEAR allows more accurate overall color tones rendering and creates more diverse reflection details on the rendered virtual spheres. The high-quality environment visual structure details contribute to the improved reflection details.

Figure 11 highlights the quantitative comparison between CLEAR and two SoTA methods [30, 41]. Overall, CLEAR achieves leading estimation accuracy than comparing methods in terms of scale-invariant RMSE on the three-sphere protocol evaluation. In Figure 11b, we show that CLEAR achieves lower lighting estimation latency than state-of-the-art methods by large margins. In particular, compared to a diffusion model-based method (DiffusionLight [30]), CLEAR takes significantly less time (110X). This reduction in estimation latency is due to CLEAR’s fewer model inferences and lower per-inference latency compared to DiffusionLight. The estimation latency reduction allows faster virtual object rendering updates and more responsive user experiences in mobile AR applications.

**6.2.4 Context Data Impact Ablation.** In Table 2, we show more comparisons between CLEAR and two state-of-the-art method [30, 41] using the three-sphere evaluation protocol. We follow the setups in [30, 41] to use a single centered view of a 75° horizontal FoV camera as input. Under the same environmental observations, CLEAR achieves lower scale-invariant and normalized RMSE values across all three virtual sphere types. Noticeably, for the mirror sphere, the sphere with the most challenging material, CLEAR achieves approximately 50% reduction in the measured scale-invariant RMSE values. On the other hand, we noticed that CLEAR generates environment maps with slightly higher angular errors. Upon further inspection, we suspect that the diverse environment map image details potentially caused the higher angular error because the angular error metric is sensitive to pixel-wise differences.

This setup configuration represents a baseline performance of CLEAR because our system can take in more AR context data during the runtime. Therefore, we conducted further comprehensive evaluations on several configurations over camera FoVs, the number of input views, and the usage of semantic maps. Note that the ambient light data has been included in all tests in Table 2 because it is inseparable from our estimation pipeline design. The added environment observations through new views and increased FoVs can both improve the accuracy of lighting estimation. Additionally, full-scene semantic maps are important guiding information for high-accuracy lighting estimation. Full-scene semantic maps can often be obtained as floor maps or scene design layouts in real-world applications. Our testing result suggests that sharing scene semantics can greatly benefit lighting estimation accuracy with our system.

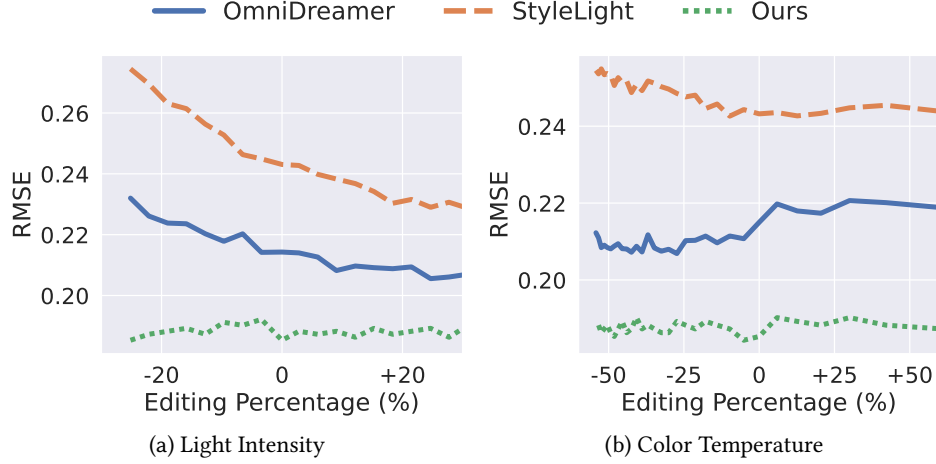


Fig. 12. Robustness testing result. We test the robustness of our lighting estimation results against two recent lighting estimation models [3, 41] using our robustness testing protocol. CLEAR shows consistently lower estimation error rates on different lighting conditions. This observation indicates CLEAR can generalize better and provide more consistent result quality in different lighting conditions.

**6.2.5 Robustness Evaluation.** We test the lighting estimation robustness of CLEAR under several environmental lighting conditions with the robustness testing protocol. For comparison, we test our system against two recent lighting estimation methods that are built on top of generative models: OmniDreamer [3] and StyleLight [41]<sup>6</sup>. The lighting estimation error rates are calculated as normalized RMSE values on estimated LDR environment maps. In Figure 12, we observe that the accuracy of both OmniDreamer and StyleLight are affected by the changing lighting intensities and color temperatures. Particularly, the lower environmental lighting intensity significantly increases the lighting estimation error rates on existing models. The observed error increases potentially are caused by the unbalanced training datasets used by these models. While CLEAR, on the other hand, shows consistently lower estimation error rates on different light intensity and color temperature conditions.

**6.2.6 Evaluation of LDR Environment Map Completion.** For the completion of the LDR environment map, we specifically examine the pixel-wise errors and the overall diversity of the environment map content. The former assesses CLEAR’s LDR lighting estimation accuracy, and the latter evaluates the generation richness of CLEAR generative estimation pipeline. When assessing the accuracy of the LDR estimation, we also include adaptive generation post-processing and candidate selection operations on the raw LDR environment map completion model output. Following [3, 41], we adopt two methods for measuring the generation content diversity: (i) calculate the FID score on the full estimated LDR environment map, and (ii) converting the environment map into a cube map and calculate FID scores on each face *without the top and bottom faces* as these two faces containing little information. In Table 3, we show that our LDR environment map completion model can output environment map images with greater diversity than state-of-the-art models. Our LDR completion model outperforms other models by 27% to 370% in the first calculation method and 4% to 344% in the second calculation method. This observation confirms the effectiveness of our large LDR environment map completion dataset. Next, we compare the accuracy of the LDR environment map completion. Under the same environment observations as [30, 41],

<sup>6</sup>We were unable to complete the robustness testing for DiffusionLight [30] within a reasonable time given its high inference cost and the large scale of data needed.

Table 3. Environment map generation diversity.

Method	FID ↓ (full env. map)	FID ↓ (selected regions)
Gardner et al. 2017 [16]	307.5	197.4
OmniDreamer [3]	<u>106.3</u>	<u>46.2</u>
StyleLight [41]	137.7	97.2
DiffusionLight [30]	207.2	193.5
Ours	<b>86.3</b>	<b>44.31</b>

Table 4. LDR environment map estimation accuracy.

Method	RMSE ↓	Si-RMSE ↓	Angular Error ↓
StyleLight [41]	0.246	0.271	<u>5.814</u>
DiffusionLight [30]	<b>0.187</b>	<u>0.303</u>	<b>4.412</b>
Ours	<u>0.195</u>	<b>0.262</b>	6.762

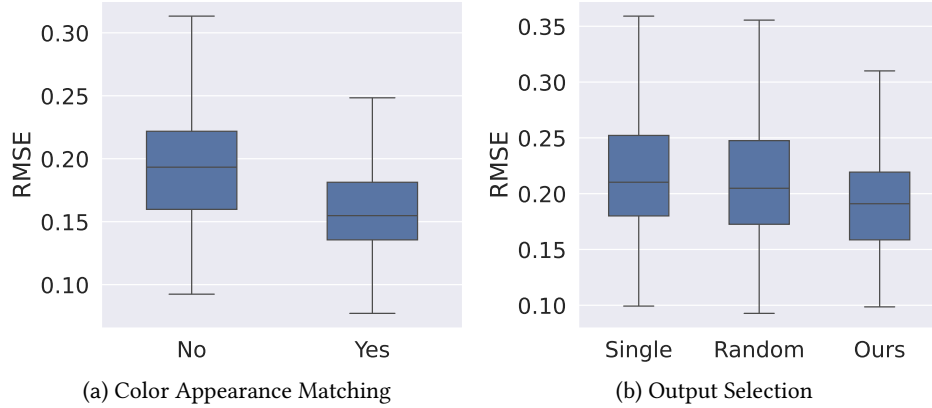


Fig. 13. Analysis of estimation refinement. (13a) Our color appearance matching technique can effectively improve overall estimation accuracy. (13b) We compare our output selection method to two straw-man baselines: single estimation output and random selection. Our method reduces the estimation of RMSE and its standard deviation compared to other baselines.

our method achieves comparable results to DiffusionLight even though our LDR completion model is based on a smaller-sized pre-trained diffusion model.

**6.2.7 Analysis of Estimation Refinement.** We evaluate the performance of our on-device estimation refinement components on the impacts of lighting estimation accuracy. In Figure 13a, we show that our color appearance matching technique improves the overall estimation accuracy by 31%. The estimation refinement technique allows our system to achieve high-quality estimation with limited estimation outputs. By default, our system only requires five generation outputs while DiffusionLight [44] requires more than 90 generation outputs. Reducing the required generation output will also reduce the estimation latency and computation resources requirements during deployment. Next, we evaluate the effectiveness of our generation output selection policy. In Figure 13b, we show that our color-matching technique can reduce the estimation error rate compared to other selection methods. We observed that, with our output selection policy and a total of five generation outputs, CLEAR can reduce 15% of the estimation error compared to using a single generation output. Furthermore, when using five generation outputs, our generation output selection component can reduce the average estimation error rate by 11% compared to random selection.



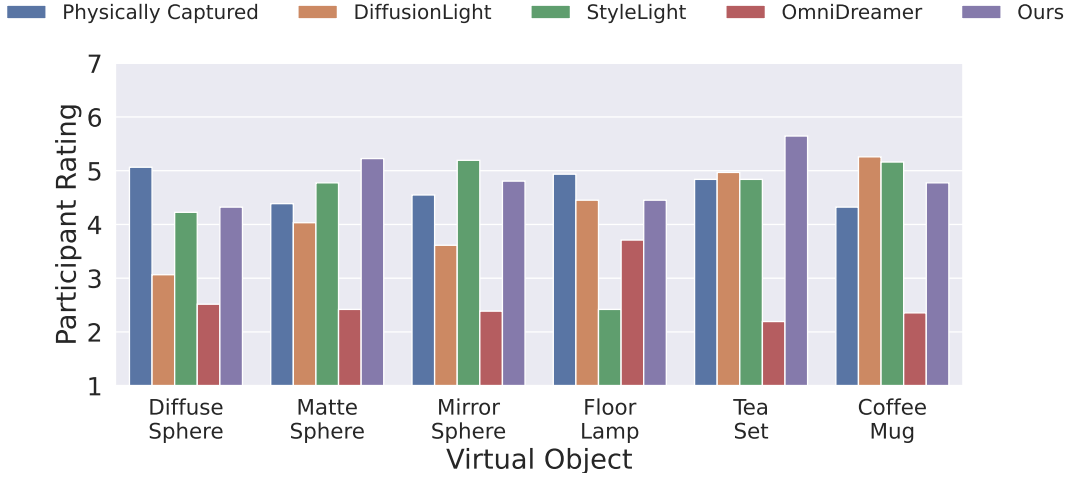


Fig. 14. Visual quality assessment user study results. We compare the virtual object rendering visual quality impacts between CLEAR and four other methods from 31 participants’ feedback in six different environments. Overall, participants report the visual quality rating of CLEAR ranked the top with an average score of 4.87, 12% higher than the second-best method, StyleLight (average score: 4.3). The overall standard deviation of the rating values for CLEAR (1.56) is also lower than StyleLight (1.67) by 7%, showing more robust estimation quality.

## 7 USER STUDY

Our user study is conducted as an online survey via the Qualtrics<sup>7</sup> platform. Our studies were approved by our organization’s Institutional Review Board (IRB) and then distributed through personal and professional networks. Participants in this study were voluntary and subject to informed consent, presented at the beginning of the survey form.

### 7.1 Study Protocol

Our study survey consists of three main chapters. The first chapter surveys the participants’ past experiences with mobile AR and their impressions of virtual object rendering qualities with existing mobile AR applications. We received responses from 31 individuals (48% female, 45% male, 6% non-binary/third gender) with varying levels of expertise in computer technology. Respondents were familiar with multiple areas of graphics technology, with image editing being the most common (51.6%). This was followed by video editing (41.9%) and 3D modeling and rendering (35.5%). 25.8% of respondents reported not being familiar with specific areas of graphics technology. 58% individuals have used AR devices. Among the respondents, mobile phones or tablets were the most commonly used devices for AR applications, with 48% having used them. Meta Quest was the second most popular device, used by 29% of the respondents.

The second chapter of our survey is a training section that guides participants in completing the quality assessment study. This chapter first shows a quality rating question where the participants will be given 5 images. Each image contains the same virtual sphere rendered by five different lighting conditions created from five sources. Participants are instructed to rate the visual qualities using a Likert scale of 1 to 7, where 1 represents the lowest quality and 7 represents the highest. Participants are not aware of which lighting sources are used and their mappings to the images. An example rating for this question is shown to the user for training purposes.

<sup>7</sup>Qualtrics: <https://www.qualtrics.com/>

Next, we will show a follow-up question to ask participants for feedback, specifically on the quality issues of images generated by our system. Following the training chapter, the third is the formal quality assessment study.

## 7.2 Results

In the formal study, we presented participants with six question groups, each with a distinctive virtual object. The question group follows the format used in the training chapter. The order of environment lighting used for generating the images is randomized and will not be shown to participants. In Figure 14, we show six groups of visual quality ratings. Each group uses different environments and virtual object setups, representing environments with varying lighting conditions and objects with various geometries and materials. Six virtual objects are used in total, including a diffuse sphere, matte sphere, mirror sphere, floor lamp, tea set, and coffee mug. Specifically, lighting conditions used in these questions were generated using CLEAR, DiffusionLight [30], StyleLight [41], OmniDreamer [3], and physically captured HDR environment maps.

Excluding the ratings of virtual objects rendered by physically captured lighting, from the collected responses, 4 out of 6 objects reported better virtual object rendering quality using environment lighting generated by CLEAR. On average, the visual quality rating of CLEAR ranked the top with an average score of 4.87 across all responses. This score is about 12% higher than the second-best method, StyleLight (average score: 4.35). Additionally, the overall standard deviation of the rating values for CLEAR (1.56) is also lower than StyleLight (1.67) by 7%, showing more robust estimation quality.

Interestingly, we found that, in two questions (tea set and coffee mug), participants' ratings suggest even better visual quality for CLEAR than the physically captured environment maps. Upon further inspection, we found that, although physically captured environment lighting represents a more accurate of the radiance conditions in the scene, human vision favors the slightly brighter outputs generated by CLEAR. We hope this finding raises new interest in the research community to design and evaluate lighting estimation systems in the future with considerations of human perception.

## 8 RELATED WORK

### 8.1 Environment Lighting and Rendering

Pioneering works have established several ways of capturing high-fidelity physical environment lighting and representing them in digital formats. Omnidirectional HDR environment map is a commonly adopted solution [12] for representing the environment lighting because it stores the incoming radiance information that can be easily integrated with modern computer graphics rendering. Environment maps can be commonly captured using mirror balls, 360° cameras, or bracketed image stitching [6, 13]. A recent work, GLEAM [31], incorporates the mirror ball-assisted environment lighting capturing process into AR applications. However, the requirement for the presence of the mirror ball limits the practicality of AR device usage. Instead, our system uses the generative estimation approach to provide flexible, high-quality lighting estimation. Additionally, HDR environment maps can be challenging to obtain on AR devices due to many sensor limitations. Recent lighting estimation systems [50, 52] can only output LDR ones. But our two-stepped generative estimation design allows CLEAR to support HDR lighting estimation.

### 8.2 Image Generative Models

Recently, generative models have demonstrated impressive capabilities in image synthesis, as well as generating audio, 3D models, and other data modalities [11, 44]. The generative diffusion model [19] receives particularly strong attention from the research community because of its high-quality outputs in image generation. The generative diffusion model uses a physical diffusion process inspired by the Gaussian signal denoising generation process. Combining this novel generation process with the large model parameter sizes, generative diffusion

models outperform generative models with prior architectures, such as GAN [18] or VAE [15]. Several recent works [3, 9, 30, 41] also propose to adopt generative models, including diffusion models, to solve the generic lighting estimation problem. In this work, we focus on solving the lighting estimation problem in the context of mobile AR applications using generative models.

### 8.3 Context-aware Mobile System

Context-aware computing is a classical computing paradigm in which applications can discover and take advantage of contextual information [8]. Early research in context-aware AR systems [38] demonstrated that important environment information can be extracted from camera frames for task planning and decision-making. In recent years, new developments of AR systems have also sought to leverage broad types of environment context information to assist several AR tasks and achieve better user experiences [24, 39, 42]. Our work uses two types of context information: environment semantics and ambient light sensor data. These context data provide important complementary information and important guidance for matching the environment map visual context and the lighting conditions between the estimated result and the physical lighting conditions.

## 9 CONCLUSIONS

In this work, we introduced an end-to-end lighting estimation framework CLEAR that can be easily integrated into many existing mobile AR applications. Specifically, our two-step generative lighting estimation pipeline ensures high-quality and robust results under multiple environmental lighting conditions, including various light intensities and color temperatures. Our novel design uses pre-trained large generative models and runtime AR environmental context data to generate HDR environment maps more accurately from limited RGB observations. Our runtime generation control components improve the quality of lighting and reduce estimation latency. Comprehensive quantitative evaluation and user study confirm the accuracy and robustness of CLEAR compared to recent generative models.

## REFERENCES

- [1] 2024. Poly Haven. <https://polyhaven.com/>. Accessed: 2024-05-01.
- [2] Mahmoud Afifi and Michael S Brown. 2020. Deep white-balance editing. In *Proceedings of the IEEE/CVF Conference on computer vision and pattern recognition*. 1397–1406.
- [3] Naofumi Akimoto, Yuhi Matsuo, and Yoshimitsu Aoki. 2022. Diverse Plausible 360-Degree Image Outpainting for Efficient 3DCG Background Creation. In *Proceedings of the IEEE/CVF Conference on Computer Vision and Pattern Recognition (CVPR)*.
- [4] Inc Apple. 2022. *Augmented Reality - Apple Developer*. Retrieved Oct 14, 2022 from <https://developer.apple.com/augmented-reality/>
- [5] Ali J Ben Ali, Marziye Kouroshli, Sofiya Semenova, Zakieh Sadat Hashemifar, Steven Y Ko, and Karthik Dantu. 2022. Edge-SLAM: Edge-assisted visual simultaneous localization and mapping. *ACM Transactions on Embedded Computing Systems* 22, 1 (2022), 1–31.
- [6] Matthew Brown and David G Lowe. 2007. Automatic panoramic image stitching using invariant features. *International journal of computer vision* 74 (2007), 59–73.
- [7] Angel Chang, Angela Dai, Thomas Funkhouser, Maciej Halber, Matthias Niessner, Manolis Savva, Shuran Song, Andy Zeng, and Yinda Zhang. 2017. Matterport3D: Learning from RGB-D Data in Indoor Environments. *International Conference on 3D Vision (3DV)* (2017).
- [8] Guanling Chen and David Kotz. 2000. A survey of context-aware mobile computing research. (2000).
- [9] Zhaoxi Chen, Guangcong Wang, and Ziwei Liu. 2022. Text2light: Zero-shot text-driven hdr panorama generation. *ACM Transactions on Graphics (TOG)* (2022).
- [10] Mathew Chylinski, Jonas Heller, Tim Hilken, Debbie Isobel Keeling, Dominik Mahr, and Ko de Ruyter. 2020. Augmented reality marketing: A technology-enabled approach to situated customer experience. *Australasian Marketing Journal* 28, 4 (2020), 374–384.
- [11] Florinel-Alin Croitoru, Vlad Hondru, Radu Tudor Ionescu, and Mubarak Shah. 2023. Diffusion models in vision: A survey. *IEEE Transactions on Pattern Analysis and Machine Intelligence* 45, 9 (2023), 10850–10869.
- [12] Paul Debevec. 2006. Image-based lighting. In *ACM SIGGRAPH 2006 Courses*. 4–es.
- [13] Paul E Debevec and Jitendra Malik. 2023. Recovering high dynamic range radiance maps from photographs. In *Seminal Graphics Papers: Pushing the Boundaries, Volume 2*. 643–652.

- [14] David Eigen, Christian Puhrsch, and Rob Fergus. 2014. Depth map prediction from a single image using a multi-scale deep network. *Advances in neural information processing systems* 27 (2014).
- [15] Patrick Esser, Robin Rombach, and Bjorn Ommer. 2021. Taming transformers for high-resolution image synthesis. In *Proceedings of the IEEE/CVF conference on computer vision and pattern recognition*. 12873–12883.
- [16] Marc-André Gardner, Kalyan Sunkavalli, Ersin Yumer, Xiaohui Shen, Emiliano Gambaretto, Christian Gagné, and Jean-François Lalonde. 2017. Learning to Predict Indoor Illumination from a Single Image. *ACM Transactions on Graphics* (2017).
- [17] Marc-André Gardner, Yannick Hold-Geoffroy, Kalyan Sunkavalli, Christian Gagné, and Jean-François Lalonde. 2019. Deep parametric indoor lighting estimation. In *Proceedings of the IEEE/CVF International Conference on Computer Vision*. 7175–7183.
- [18] Ian Goodfellow, Jean Pouget-Abadie, Mehdi Mirza, Bing Xu, David Warde-Farley, Sherjil Ozair, Aaron Courville, and Yoshua Bengio. 2020. Generative adversarial networks. *Commun. ACM* 63, 11 (2020), 139–144.
- [19] Jonathan Ho, Ajay Jain, and Pieter Abbeel. 2020. Denoising diffusion probabilistic models. *Advances in neural information processing systems* 33 (2020), 6840–6851.
- [20] Weixiang Hong, Zhenzhen Wang, Ming Yang, and Junsong Yuan. 2018. Conditional generative adversarial network for structured domain adaptation. In *Proceedings of the IEEE conference on computer vision and pattern recognition*. 1335–1344.
- [21] Noor A Ibraheem, Mokhtar M Hasan, Rafiqul Z Khan, and Pramod K Mishra. 2012. Understanding color models: a review. *ARPJ Journal of science and technology* 2, 3 (2012), 265–275.
- [22] Yi Jiang, Xueqin Wang, and Kum Fai Yuen. 2021. Augmented reality shopping application usage: The influence of attitude, value, and characteristics of innovation. *Journal of Retailing and Consumer Services* 63 (2021), 102720.
- [23] Diederik P Kingma. 2013. Auto-encoding variational bayes. *arXiv preprint arXiv:1312.6114* (2013).
- [24] Kit Yung Lam, Lik Hang Lee, and Pan Hui. 2021. A2w: Context-aware recommendation system for mobile augmented reality web browser. In *Proceedings of the 29th ACM international conference on multimedia*. 2447–2455.
- [25] Chloe LeGendre, Wan-Chun Ma, Graham Fyfe, John Flynn, Laurent Charbonnel, Jay Busch, and Paul Debevec. 2019. Deeplight: Learning illumination for unconstrained mobile mixed reality. In *Proceedings of the IEEE Conference on Computer Vision and Pattern Recognition*. 5918–5928.
- [26] Zhengqin Li, Li Yu, Mikhail Okunev, Manmohan Chandraker, and Zhao Dong. 2023. Spatiotemporally consistent hdr indoor lighting estimation. *ACM Transactions on Graphics* 42, 3 (2023), 1–15.
- [27] Mehdi Mirza. 2014. Conditional generative adversarial nets. *arXiv preprint arXiv:1411.1784* (2014).
- [28] Hiroki Noguchi and Toshihiko Sakaguchi. 1999. Effect of illuminance and color temperature on lowering of physiological activity. *Applied human science* 18, 4 (1999), 117–123.
- [29] Yoshi Ohno. 2014. Practical use and calculation of CCT and Duv. *Leukos* 10, 1 (2014), 47–55.
- [30] Pakkapon Phongthawee, Worameth Chinchuthakun, Nontaphat Sinsunthithet, Amit Raj, Varun Jampani, Pramook Khungurn, and Supasorn Suwajanakorn. 2023. DiffusionLight: Light Probes for Free by Painting a Chrome Ball. In *ArXiv*.
- [31] Siddhant Prakash, Alireza Bahremand, Linda D Nguyen, and Robert LiKamWa. 2019. Gleam: An illumination estimation framework for real-time photorealistic augmented reality on mobile devices. In *Proceedings of the 17th Annual International Conference on Mobile Systems, Applications, and Services*. 142–154.
- [32] Philipp A Rauschnabel, Reto Felix, and Chris Hinsch. 2019. Augmented reality marketing: How mobile AR-apps can improve brands through inspiration. *Journal of Retailing and Consumer Services* 49 (2019), 43–53.
- [33] Scott Reed, Zeynep Akata, Xinchun Yan, Lajanugen Logeswaran, Bernt Schiele, and Honglak Lee. 2016. Generative adversarial text to image synthesis. In *International conference on machine learning*. PMLR, 1060–1069.
- [34] Robin Rombach, Andreas Blattmann, Dominik Lorenz, Patrick Esser, and Björn Ommer. 2021. High-Resolution Image Synthesis with Latent Diffusion Models. *arXiv:2112.10752* [cs.CV]
- [35] Michelangelo Scorpio, Roberta Laffi, Ainoor Teimoorzadeh, Giovanni Ciampi, Massimiliano Masullo, and Sergio Sibilio. 2022. A calibration methodology for light sources aimed at using immersive virtual reality game engine as a tool for lighting design in buildings. *Journal of Building Engineering* 48 (2022), 103998.
- [36] Maximilian Seitzer. 2020. pytorch-fid: FID Score for PyTorch. <https://github.com/mseitzer/pytorch-fid>. Version 0.3.0.
- [37] Gowri Somanath and Daniel Kurz. 2021. HDR Environment Map Estimation for Real-Time Augmented Reality. <https://arxiv.org/pdf/2011.10687.pdf>
- [38] Thad Starner, Bernt Schiele, and Alex Pentland. [n. d.]. Visual contextual awareness in wearable computing. In *Digest of Papers. Second International Symposium on Wearable Computers (Cat. No. 98EX215)*.
- [39] Tomu Tahara, Takashi Seno, Gaku Narita, and Tomoya Ishikawa. 2020. Retargetable AR: Context-aware augmented reality in indoor scenes based on 3D scene graph. In *2020 IEEE International Symposium on Mixed and Augmented Reality Adjunct (ISMAR-Adjunct)*. IEEE, 249–255.
- [40] Aaron Van Den Oord, Sander Dieleman, Heiga Zen, Karen Simonyan, Oriol Vinyals, Alex Graves, Nal Kalchbrenner, Andrew Senior, Koray Kavukcuoglu, et al. 2016. Wavenet: A generative model for raw audio. *arXiv preprint arXiv:1609.03499* 12 (2016).

- [41] Guangcong Wang, Yinuo Yang, Chen Change Loy, and Ziwei Liu. 2022. StyleLight: HDR Panorama Generation for Lighting Estimation and Editing. In *European Conference on Computer Vision (ECCV)*.
- [42] Tianyi Wang, Xun Qian, Fengming He, Xiyun Hu, Ke Huo, Yuanzhi Cao, and Karthik Ramani. 2020. CAPturAR: An augmented reality tool for authoring human-involved context-aware applications. In *Proceedings of the 33rd Annual ACM Symposium on User Interface Software and Technology*. 328–341.
- [43] Tete Xiao, Yingcheng Liu, Bolei Zhou, Yuning Jiang, and Jian Sun. 2018. Unified perceptual parsing for scene understanding. In *Proceedings of the European conference on computer vision (ECCV)*. 418–434.
- [44] Ling Yang, Zhilong Zhang, Yang Song, Shenda Hong, Runsheng Xu, Yue Zhao, Wentao Zhang, Bin Cui, and Ming-Hsuan Yang. 2023. Diffusion models: A comprehensive survey of methods and applications. *Comput. Surveys* 56, 4 (2023), 1–39.
- [45] Yizhou Yu, Paul Debevec, Jitendra Malik, and Tim Hawkins. 1999. Inverse global illumination: Recovering reflectance models of real scenes from photographs. In *Proceedings of the 26th annual conference on Computer graphics and interactive techniques*. 215–224.
- [46] Lvmin Zhang, Anyi Rao, and Maneesh Agrawala. 2023. Adding conditional control to text-to-image diffusion models. In *Proceedings of the IEEE/CVF International Conference on Computer Vision*. 3836–3847.
- [47] Wenliang Zhao, Lujia Bai, Yongming Rao, Jie Zhou, and Jiwen Lu. 2024. Unipc: A unified predictor-corrector framework for fast sampling of diffusion models. *Advances in Neural Information Processing Systems* 36 (2024).
- [48] Yiqin Zhao, Sean Fanello, and Tian Guo. 2023. Multi-camera lighting estimation for photorealistic front-facing mobile augmented reality. In *Proceedings of the 24th International Workshop on Mobile Computing Systems and Applications*. 68–73.
- [49] Yiqin Zhao and Tian Guo. 2020. Pointar: Efficient lighting estimation for mobile augmented reality. In *European Conference on Computer Vision*. Springer, 678–693.
- [50] Yiqin Zhao and Tian Guo. 2021. Xihe: A 3D Vision-Based Lighting Estimation Framework for Mobile Augmented Reality. In *Proceedings of the 19th Annual International Conference on Mobile Systems, Applications, and Services (MobiSys'21)*. 13 pages.
- [51] Yiqin Zhao and Tian Guo. 2024. Demo: ARFlow: A Framework for Simplifying AR Experimentation Workflow. In *Proceedings of the 25th International Workshop on Mobile Computing Systems and Applications* (, San Diego, CA, USA,) (*HOTMOBILE '24*). Association for Computing Machinery, New York, NY, USA, 154. <https://doi.org/10.1145/3638550.3643617>
- [52] Yiqin Zhao, Chongyang Ma, Haibin Huang, and Tian Guo. 2022. LITAR: Visually Coherent Lighting for Mobile Augmented Reality. *Proceedings of the ACM on Interactive, Mobile, Wearable and Ubiquitous Technologies* 6, 3 (2022), 1–29.
- [53] Jia Zheng, Junfei Zhang, Jing Li, Rui Tang, Shenghua Gao, and Zihan Zhou. 2020. Structured3d: A large photo-realistic dataset for structured 3d modeling. In *Computer Vision–ECCV 2020: 16th European Conference, Glasgow, UK, August 23–28, 2020, Proceedings, Part IX* 16. Springer, 519–535.
- [54] Bolei Zhou, Hang Zhao, Xavier Puig, Sanja Fidler, Adela Barriuso, and Antonio Torralba. 2017. Scene parsing through ade20k dataset. In *Proceedings of the IEEE conference on computer vision and pattern recognition*. 633–641.